Chapter- 2

Adsorption and Photocatalytic Degradation Studies of Methylene Blue on Sol –Gel Derived CdS -Ti MCM-41

K. Fasna, V.P Fathima Shahana,
Dr. K.P. Sreenivasan *
Centre for Sustainable Chemical Research, University of Calicut
Approved Research Centre, MES Kalladi College,
Mannarkkad- 678583, Kerala, India
Corresponding author Tel: 9947753498
E-mail address : drsreenivasan@meskc.ac.in

Abstract

We suggested a simple method for the synthesis of CdS modified Ti MCM-41 catalyst materials by sol- gel method and studied the calcined materials were well characterized by Powder X-ray Diffraction, Ultraviolet-Visible diffuse reflectance spectroscopic analysis, ATR FT-IR Spectroscopy, N_2 Sorption analysis and transmission Electron Microscopy. The powder X -ray diffraction data showed the presence of hexagonal phase CdS and variation in crystallinity of the material as we changed the composition of the materials. Upon increasing the amount of CdS concentration, the intensity of the spectra in the visible region also increased. From transmission electron microscopy analysis, noticed the presence of CdS nanoparticle along with TiO_2. The textural properties of CdS modified Ti MCM 41 was found to be lower than that of the parent Ti MCM41. Up on studying the photocatalytic activity of the material, CdS modified Ti MCM 41 showed lower photocatalystic activity under direct sunlight irradiation. This might be attributed to lower surface area, crystallinity, and visible light sensitivity of the CdS modified Ti MCM 41.

Keywords: Sol- gel method, mesoporous material, TM -41, CdS modification, Photodegradation, methylene blue

1. Introduction

Meso structured silica, like MCM-41, has small pore size distributions, high surface areas, and organised frameworks, making it the most suitable support [1-3]. However, the visible light supported photocatalytic performance of mesoporous silica-TiO_2 is very poor. Therefore, structural and surface modification of TiO_2 is necessary for improving visible light absorption capacity and thereby enhancing the efficiency of photocatalyst. An efficient photocatalyst consisting of Cd chalcogenide nanoparticle dispersed mesoporous silica-titania mixed oxide materials are efficient photocatalyst for discolouration of textile effluent [4]. Material scientists are always trying to find out the most efficient photocatalysts that is visible light activated, chemically or photochemically stable and low cost[5]. Cadmium sulfide has garnered significant attention as a promising visible light-driven photocatalyst due to its narrow band gap (2.4 eV), high absorption coefficient and suitable conduction and valence band positions [6,7]. The sol-gel method was employed for the preparation of TM-41-CdS nanocomposite. Here we are trying to explore the applications of this kind of material by studying photocatalytic degradation of methylene blue.

2. Experimental

2.1 Chemicals required

Cetyl trimethyl ammonium bromide (CTAB) (Labochemie), Titanium isopropoxide (Aldrich 98 %), Tetra ethyl ortho silicate (TEOS) (Aldrich), aqueous ammonia, Isopropyl alcohol, Cadmium acetate and sodium sulphide (Nice chemicals), Distilled water.

2.2 Preparation of Ti MCM 41

About 0.75g of CTAB was added to 15 ml of deionised water under vigorous stirring in a 250 ml beaker. After CTAB was completely dispersed in water, 17.5 ml of aqueous NH_3 was poured into the clear solution. About 23 ml isopropyl alcohol was added to the surfactant solution under vigorous stirring. After stirring for 30 minutes, 3 ml TEOS was added and stirred continuously for further 30 minutes. Then 2.2 ml titanium isopropoxide was added slowly to the solution during stirring. The resultant gel was kept for drying at room temperature. Calcination

ISBN: 9789348505767

was done at 550^0C in a static air environment. The obtained sample was labelled as TM 41.

2.3. Preparation of CdS modified Ti MCM 41

For the preparation of the CdS -modified Ti MCM 41, 0.5g of previously prepared TM 41 was added to 10 ml of water. After stirring for 30 minutes add 80 mg of cadmium acetate into it. After stirring for 15 minutes, 0.02 g of sodium sulphide in 10 ml of water was added to in it. The resultant mixture was keep drying for 5 days and then washed with 500 ml water. The samples obtained were dried in static atmosphere. The sample was labeled as TM 41- CdS- 80. The same procedure was repeated with 160 mg, 40 mg of cadmium acetate and 20 mg of sodium sulphide respectively to obtain TM 41- CdS-160, TM 41-CdS-40 respectively.

2.4 Characterization

The XRD measurements were performed at room temperature using a Rigaku Ultima IV X-ray diffractometer with Cu Kα radiation. The diffractometer was operated at 40 kV, and 44 mA, scanned with a step size of 0.02°, and a count time of 1°/min in the range of 2θ angle 10 to 80. The FT-IR analysis were carried out using a Bruker ALPHA instrument with ATR Pt diamond holder and the spectra were acquired in the range 4000 cm^{-1} to 500 cm^{-1} with a resolution of 4cm^{-1} The TEM images were recorded on a HRTEM Jeol/JEM 2100 instrument operating at 200 kV. Prior to TEM analysis, the sample was dispersed in ethanol and the suspension was sonicated for 1h. For each material, one drop of suspension was placed on a copper grid coated with carbon film, and allowed to dry overnight. The textural properties, such as surface area and pore size distribution of TM 41 and as TM 41-CdS 160 materials were analyzed by using N_2 physisorption measurements. After the samples are dried overnight at 70 °C and degas at 200 °C for at least 1 h, N_2 isotherms are obtained at -196 °C using a BELSORP-max surface area and pore size analyzer. The surface areas of the synthesized materials were calculated by using the Brunauer-Emmett-Teller (BET) equation within a relative pressure range (P/P_0) of 0.05–0.30. The pore volume was determined from the amount of N_2 adsorbed at the highest relative pressure of P/P0

ISBN: 9789348505767

≈ 0.99. The pore diameter and pore size distribution plots are defined by applying the Barrett-Joyner-Halenda (BJH) model to the desorption isotherm. The UV-Vis diffuse spectra were recorded by a JascoV-550 UV-Visible spectrophotometer with Jasco model ISV 469 reflection accessory.

3. Results and discussion

3.1 Powder XRD Analysis

The powder XRD patterns of the materials TM 41, TM 41- CdS- 40, TM 41- CdS- 80, and TM 41- CdS- 160, were shown in Fig.1**.** All the mesoporous materials showed a fairly broad peak between 2θ values of 20 and 30. This is typical of amorphous silica support. The broad peaks due to TiO_2 and CdS indicated that both of these species were highly dispersed on the mesoporous silica support. This suggested that the TiO_2 and the CdS were amorphous in nature. Upon modification of TM 41 with CdS nanoparticle a new peak at 17 appeared. Peaks due to d_{100}, d_{002}, d_{101}, d_{110}, d_{103}, and d_{112}, at 25.6, 26.4, 30.1, 43.7, 48.2 (overlapping with TiO_2), and 52.0, indicated that the hexagonal phase of CdS [8].

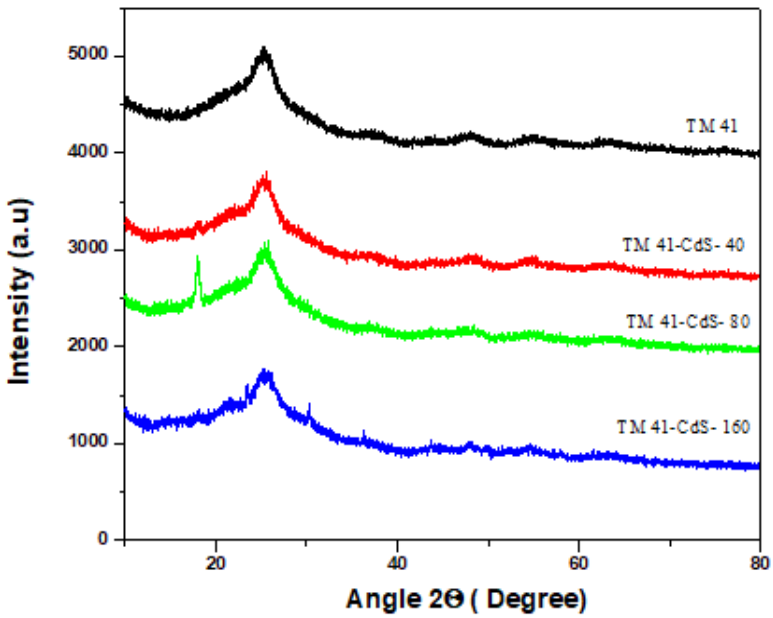

Fig .1 XRD patterns of TM41, TM 41-CdS-40, TM41-CdS- 80, Tm 41-CdS-160 respectively

ISBN: 9789348505767

3.2 UV-Visible DRS Analysis

UV-Visible diffuse reflectance spectroscopic analysis was carried out to knowing the optical properties of the materials. The UV-Vis spectra of TM41, TM41-CdS-80, TM41-CdS-160, and TM41-CdS-40 were shown in Fig .2. All the CdS modified samples showed a broad bands between 400 and 500 nm corresponding to band gap absorption of CdS [9, 10]. Intensity of the band increased with concentration of CdS precursor. Two types of absorption onsets, one in the UV and another in the visible region were seen. These distinct absorption bands were due to the presence of CdS and TiO_2 species, respectively.

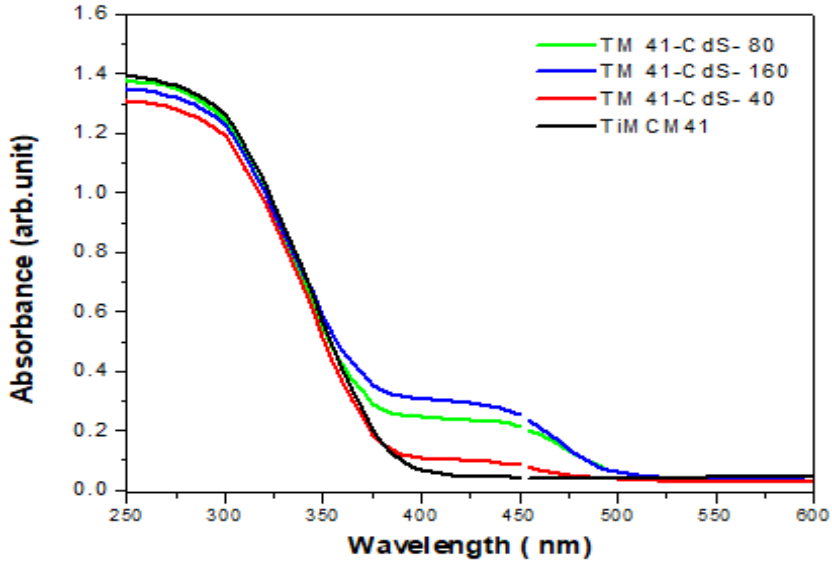

Fig .2 UV-Vis spectra of TM41, TM 41-CdS-40, TM41-CdS- 80, Tm 41-CdS-160 respectively

3.3 ATR-FT-IR Spectroscopy

In order to acquire information about the different functional groups, the materials were further characterized by using FT-IR analysis. The spectrum was shown in Fig.3. All the samples showed typical IR spectra of TM 41 as reported earlier. It was reported that the characteristic broad peak for Si-O-Si observed in between 900-1200 cm^{-1}, while the peak observed at 870 cm^{-1} was due to Si-O-Si symmetric stretching. The broad peak observed at 1600 cm^{-1} was due to OH bending vibrations and is attributed to chemisorbed water molecules [11].

ISBN: 9789348505767

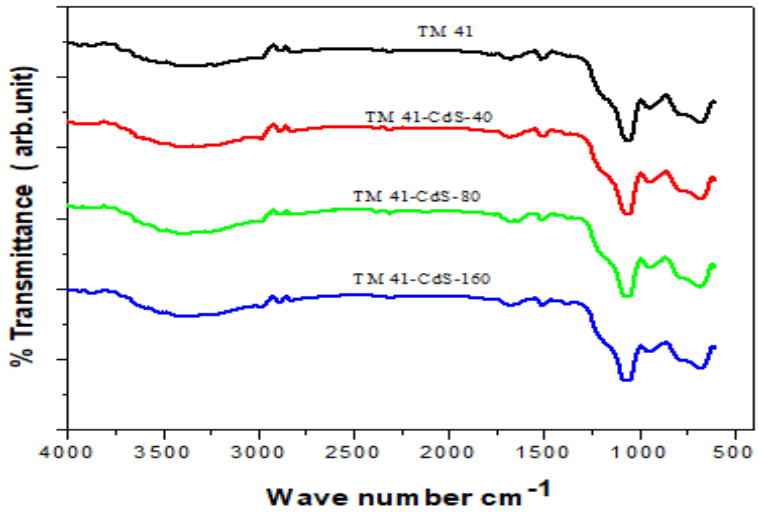

Fig.3. ATR FT-IR spectra of TM 41, TM 41-CdS-40, TM41-CdS- 80, Tm 41-CdS-160 respectively

3.4 TEM Analysis

TEM images of TM 41 and representative material TM 41 -CdS-160 were shown in Fig. 4. From the TEM images of TM 41 and representative material, TM 41-CdS-160, the TiO_2 particles were randomly distributed with a particle size of 10-15 nm. The TEM image of TM 41 CdS-160 showed lattice fringes due to CdS nanoparticle [10].

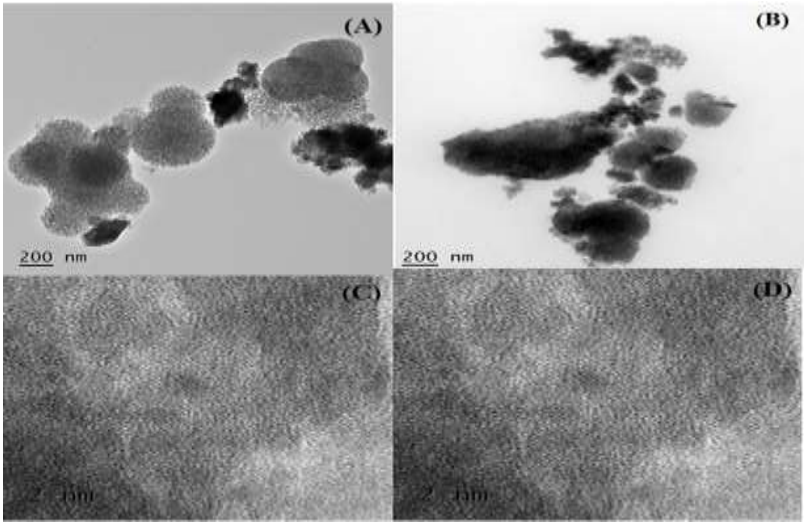

Fig. 4. TEM images of TM41 (A, C) and TM 41-CdS-160 (B, D)

ISBN: 9789348505767

3.5 Nitrogen physisorption studies

The N_2 isotherms and pore size distribution curve of TM41-CdS-160, TM 41 prepared in these studies were shown in Fig. 3.5. The N_2 isotherms of TM41 and TM41-CdS-160 indicated that, the materials exhibited type IV isotherms typical of mesoporous materials. The hysteresis loops featured in the isotherms were reflection of porosity of these materials. The initial part of type IV isotherm was due to monolayer adsorption at low relative pressures. As the relative pressure increases, multilayer adsorption occurs followed by capillary condensation. The material TM41-CdS-160 and TM41 suggested a set of pores with a BJH pore diameters of 8.2 nm and 3.65 nm respectively. The textural property details of these materials were also shown in Table 1.

Table 1. Textural properties of TM41 and TM41-CdS-160

Materials	Specific surface area m^2/g	Pore diameter(nm)	Pore volume
TM41-CdS-160	22.55	8.2	0.04
Ti MCM41 (TM 41)	385	3.65	0.35

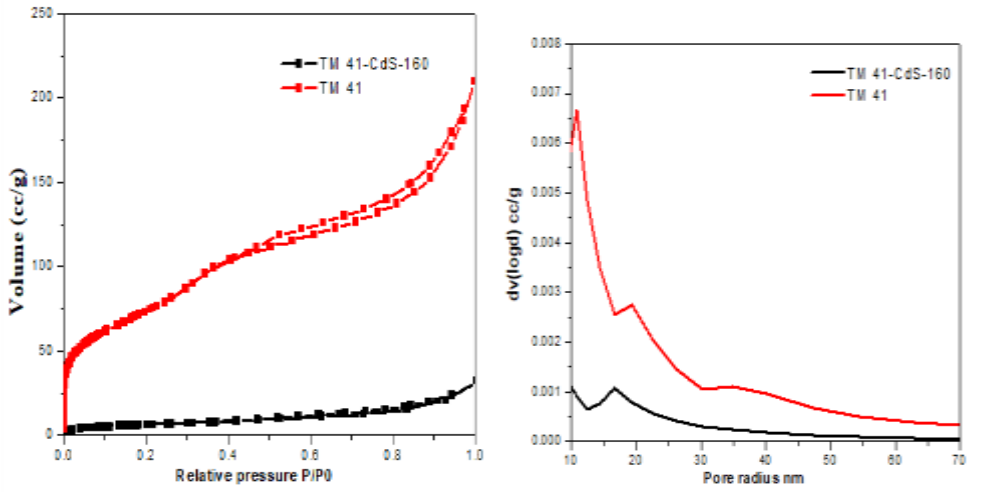

Fig.5. N_2 isotherms and pore size distribution curve of TM 41 and TM41-CdS-160

The TM-41 having the surface area 385 cm^{-1} showing type IV behaviour with H3 type hysteresis loop have an average pore diameter of 3.65 nm and pore volume 0.35cm^3g^{-1} which was shown in Fig. 5 and in

ISBN: 9789348505767

Table 1. This study indicated that upon modification with the CdS nanoparticle the surface area of the TM -41 has been reduced and is more prominent.

3.6 Adsorption studies of dye molecule.

Absorbance corresponding to methylene blue and methylene blue unabsorbed on catalyst materials at same interval of time were shown in Fig.6. The plot corresponding to the absorbance of methylene blue using TM 41 was lower compared to TM41-CdS-40, TM41-CdS 80, TM41-CdS-160) materials. Which, indicated that maximum amount of dye species were adsorbed on TM 41surface. Upon modification with CdS nanoparticle absorbance of methylene blue was slightly higher compared to TM 41 sample [13].

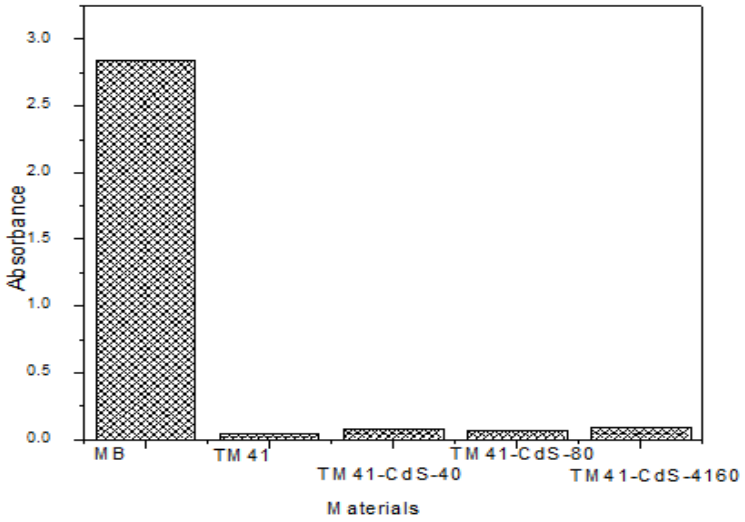

Fig. 6. Adsorption properties of methylene blue over TM41, TM41-CdS-40, TM41-CdS 80, TM41-CdS-160 respectively

3.7 Phocatalytic degradation studies

UV/ Visible Absorbtion spectra corresponding to methylene blue degraded on catalyst materials at same interval of time were shown in Fig. 6. The absorbance of methylene blue corresponding to the λ_{max} was lowered in presence of TM 41 compared to TM41-CdS-40, TM41-CdS 80, TM41-CdS-160 materials which indicated that maximum amount of dye species were degraded by TM41 material by photocatalytic reaction.

ISBN: 9789348505767

Upon treatment with CdS modified materials TM41-CdS-40, TM41-CdS 80, TM41-CdS-160 the absorbance of methylene blue was slightly higher compared to TM41, which also indicated the controlled modification cause degradation of dye molecule on catalyst surface [14].

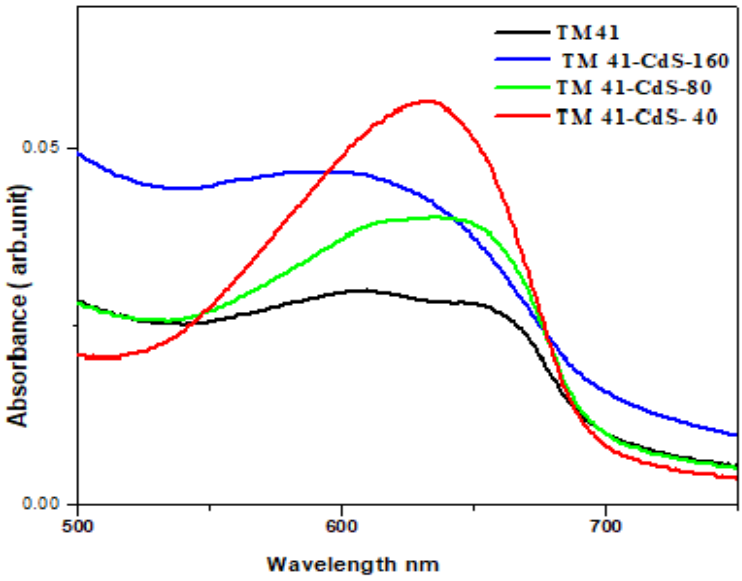

Fig.7. Phocatalytic degradation of methylene blue over TM41, TM41-CdS-40, TM41-CdS 80, TM41-CdS-160 respectively

4. Conclusion

The TM 41 nanomaterial with CdS modification was successfully done by sol-gel process. X ray diffraction analysis indicated that the synthesised material consists of anatase phase TiO_2. The UV-Vis DRS spectra of the synthesized material indicated band width intensity increased with increasing concentration of the CdS. From the TEM images, we observed that the TiO_2 particles are randomly distributed with a particle size of 10-15 nm. From photocatalytic studies it was proved that upon modification with CdS nanoparticle absorbance of methylene blue was slightly higher compared to TM 41.Through the surface area studies we could identify that the textural properties of the material was lowered upon modification with CdS. This work provided an insight to explore various method and their effects on the physico-chemical properties of mesoporous materials.

ISBN: 9789348505767

Acknowledgement:

The authors are thankful to Sophisticated Test and Instrumentation Centre (STIC) for the TEM analysis and Central Sophisticated Instrument Facility (CSIF) for the surface area analysis, and XRD. The authors would also like to acknowledge Miss Sharanya, Research Scholar, MES KVM College, Valanchery for the FT-IR and UV/Visible spectral Analysis and to Dr. Ramani, for supervising adsorption and photocatalytic degradation studies at SNGS Pattambi.

References

1. L. Chmielarz, A. Jankowska, Mesoporous silica based catalysts for selective catalytic reduction of NO_x with ammonia, Advances in Inorganic Chemistry, 79 (2022) 209-245 https://doi.org/10.1016/bs.adioch.2021.12.007
2. K. Lan, D. Zhao, Functional ordered mesoporous materials: present and future, Nano Letters 22 (2022**),** 3177–3179 https://doi.org/10.1021/acs.nanolett.2c00902
3. S. Kumar, A.Sharma, D. Gautham, S.Hooda, Advanced Functional Porous Materials. Engineering Materials. Springer, Cham (**2022)**.
4. Nidhi Gaur, Swati Sharma, Nidin Yadav, Green Chemistry Approaches to Environmental Sustainability (2024)
5. S. Rasalingham, R.Peng, R.T. Koodali, Removal of Hazardous Pollutants from Wastewaters: Applications of TiO_2 – SiO_2 Mixed Oxide Materials, Journal of Nanomaterials 2014 (2014**)**, 617405 https://doi.org/10.1155/2014/617405
6. D.Zhao, Q. Wu, CYang, R.T Koodali, Visible light driven photocatalytic hydrogen evolution over CdS incorporated mesoporous silica derived from MCM-48, Applied Surface Science, 56 (2015)308-316 https://doi.org/10.1016/j.apsusc.2015.08.008
7. R. Peng, C.M. Wu, J. Baltrusaitis, N. M. Dimitrijevic, T. Rajh, R. T. Koodali, Ultra-stable CdS incorporated Ti-MCM-48 mesoporous materials for efficient photocatalytic decomposition of water under visible light illumination, Chemical Communications, 49 (2013) 3221-3223 https://doi.org/10.1039/C3CC41362D
8. R.R. Alani, O.A. Ibrahim, Effect of point defects on the structural and optical properties of CdS nanoparticles synthesized by chemical

method, International Journal of Mechanical Engineering ,7 (2022) 5156-5165

9. M.V. Swapna, K.R. Haridas, An easier method of preparation of mesoporous anatase TiO_2 nanoparticles via ultrasonic irradiation, Journal of experimental nanoscience, 7(2016) 540-549. https://doi.org/10.1080/17458080.2015.1094189
10. S.Veeranarayanan, S. Mohammed, A. Cheruvathor , Synthesis and application of luminescent single CdS quantum dot encapsulated silica nanoparticles directed for precision optical bioimaging, International Journal of Nano medicine (2012),3769-86. https://doi.org/10.2147/IJN.S31310
11. T. Blasco, A.Corma, M.T.Navarro, J P.Pariente , Synthesis, characterization, and catalytic activity of Ti-MCM-41 structures, Journal of Catalysis, 156 (1995) 65-74 https://doi.org/10.1006/jcat.1995.1232
12. J.He, W. P. Xu, D. G.Evans, X. Duan, C. Y. Li, Role of pore size and surface properties of Ti-MCM-41 catalysts in the hydroxylation of aromatics in the liquid phase, Microporous and Mesoporous materials, 44-45 (2001)**,** 581-586 https://doi.org/10.1016/S1387-1811(01)00237-2
13. Y.M. Slokar, M. Marechal, Methods of decoloration of textile wastewaters, Dyes and Pigments, Journal of Chemistry (1998), 335-356 https://doi.org/10.1016/S0143-7208(97)00075-2
14. K. Zhou, X. D. Xie, C. T. Chang, Photocatalytic degradation of tetracycline by Ti-MCM-41 prepared at room temperature and biotoxicity of degradation products Applied Surface Science , 416 (2017), 248-258. https://doi.org/10.1016/j.apsusc.2017.04.174

ISBN: 9789348505767